

# Temperature Dependence of Transfer Properties: Importance of Heat Capacity Effects

Collin D. Wick,<sup>†</sup> J. Ilja Siepmann,<sup>\*,†</sup> and Mark R. Schure<sup>‡</sup>

Departments of Chemistry and of Chemical Engineering and Materials Science, University of Minnesota, 207 Pleasant Street SE, Minneapolis, Minnesota 55455, and Theoretical Separation Science Laboratory, Rohm and Haas Company, 727 Norristown Road, P.O. Box 0904, Spring House, Pennsylvania 19477

Received: November 1, 2002; In Final Form: May 5, 2003

Gibbs ensemble Monte Carlo simulations were used to calculate precisely the Gibbs free energies, enthalpies, and entropies of transfer for water, 1-butanol, and *n*-octane between their own liquid phase and a helium vapor phase. It is observed that the temperature dependence of the enthalpy of transfer (i.e., the heat capacity of transfer), and not the temperature–entropy term, dominates the temperature dependence of the Gibbs free energy of transfer. Nevertheless, the curvature induced by the heat capacity in a van't Hoff plot is small, and the van't Hoff equation yields an enthalpy of transfer close to the value calculated directly at the mean temperature.

## Introduction

Temperature is one of the most often used parameters to control solution processes, including protein folding or complexation or DNA/RNA denaturation,<sup>1,2</sup> liquid–liquid extraction,<sup>3</sup> and chromatographic separations.<sup>4</sup> Despite its ubiquitous use, however, there is incomplete understanding of the factors that govern the effect of temperature on solution free energies (Gibbs free energies of transfer), and a common assumption is that the temperature prefactor in the entropic term dominates the overall temperature dependence. Accordingly, a linear fit in a “van't Hoff plot” is often employed to extract an enthalpy that is viewed to be constant over the temperature range of interest.

It is the goal of this work to precisely determine Gibbs free energies, enthalpies, and entropies for vapor-to-liquid transfers over a moderate temperature range to test the applicability of the van't Hoff equation and to investigate the structural changes in the solvent phase that cause the temperature dependence. For this investigation, three liquid solvents were chosen that have similar experimental normal boiling points: nonpolar *n*-octane, moderately polar 1-butanol, or highly polar water. In all three cases, helium was used for the gas phase.

## Simulation Methods

Molecular simulation, and specifically Gibbs ensemble Monte Carlo (GEMC),<sup>5</sup> is an attractive tool for the determination of many thermodynamic properties. While the underlying model (or force field) affects the accuracy of the results obtained from the simulations, the GEMC method itself introduces no further approximations, allowing for the exact determination of the Gibbs free energy, enthalpy, and entropy of transfer for a given force field. Furthermore, analysis of the simulation trajectories enables us to examine the microscopic factors that contribute to changes of the bulk thermodynamic properties.

The GEMC method makes use of multiple simulation boxes containing, say, a vapor and a liquid phase that are in thermodynamic contact but without an explicit interface. In

addition to the usual translational, rotational, and conformational moves, particle swap and volume exchange moves are employed to reach phase and mechanical equilibrium, respectively. The simulations described here are carried out in the constant-pressure version of the Gibbs ensemble; that is, the volume trial moves involve an exchange with an external pressure reservoir and are performed separately for each simulation box.<sup>5b</sup> Configurational-bias Monte Carlo (CBMC) strategies<sup>6</sup> are used to improve the acceptance rates for particle swap moves; that is, an entire solvent molecule (*n*-octane, 1-butanol, or water) or helium is transferred in a single Monte Carlo move between the two phases. The acceptance rule for the particle swap move ensures that in equilibrium the chemical potential of each species is the same in both phases.<sup>5</sup>

The united-atom version of the transferable potential for phase equilibria (TraPPE-UA) force field<sup>7</sup> was used for helium, *n*-octane, and 1-butanol, and the TIP5P model<sup>8</sup> was used for water. A spherical potential truncation at 14 Å and analytical tail corrections were used for the Lennard-Jones interactions. In addition, an Ewald sum with tin-foil boundary conditions ( $\kappa \times L = 5$  and  $K_{\max} = 5$ ) was used to treat the long-range electrostatic interactions.

The systems were composed of 200 *n*-octane, 200 1-butanol, or 300 water molecules and 100 helium atoms in most cases with the exception of the simulations at the highest temperature for *n*-octane and water (close to their normal boiling points), for which only 5 helium atoms were used. Four different temperatures (see Table 1), which span about 75 K and fall within the liquid range of these solvents, were studied at a pressure of 101.5 kPa. The temperature range for a given solvent is limited by its normal boiling point at the upper end and by the relatively low acceptance probabilities for particle swap moves at the lower end (which lead to larger statistical uncertainties). The normal boiling points for the solvent/force field combinations were calculated from additional constant-volume GEMC simulations for the neat solvents and are  $388 \pm 2$  K for *n*-octane,  $395 \pm 1$  K for 1-butanol, and  $348 \pm 1$  K for water; that is, the calculated values deviate from experiment by  $-2.5\%$ ,  $+1.0\%$ , and  $-6.7\%$ .

Ten independent simulations with production periods of 50 000 MC cycles were carried out for each system, and

\* Corresponding author. E-mail: siepmann@chem.umn.edu.

<sup>†</sup> University of Minnesota.

<sup>‡</sup> Rohm and Haas Company.

**TABLE 1: Comparison of Gibbs Free Energies, Enthalpies, and Entropies of Vapor-to-Liquid Transfer**

solute	$T$ [K]	$\Delta G$ [kJ/mol]	$\Delta H$ [kJ/mol]	$\Delta S$ [J/mol·K]
<i>n</i> -octane	298.15	-20.97 <sub>15</sub>	-37.84 <sub>5</sub>	-56.6 <sub>2</sub>
	323.15	-19.48 <sub>9</sub>	-36.47 <sub>9</sub>	-52.6 <sub>4</sub>
	348.15	-18.29 <sub>7</sub>	-34.96 <sub>12</sub>	-47.9 <sub>5</sub>
	373.15	-17.03 <sub>10</sub>	-33.39 <sub>13</sub>	-43.8 <sub>4</sub>
	van't Hoff eq		-36.8 <sub>1,1</sub>	
1-butanol	273.15	-27.54 <sub>55</sub>	-53.68 <sub>8</sub>	-95.7 <sub>20</sub>
	298.15	-25.10 <sub>24</sub>	-51.90 <sub>13</sub>	-89.9 <sub>6</sub>
	323.15	-23.07 <sub>10</sub>	-50.23 <sub>10</sub>	-84.0 <sub>4</sub>
	348.15	-21.02 <sub>10</sub>	-47.64 <sub>18</sub>	-76.5 <sub>7</sub>
	van't Hoff eq		-49.0 <sub>2,2</sub>	
water	273.15	-25.30 <sub>13</sub>	-45.48 <sub>3</sub>	-73.9 <sub>2</sub>
	298.15	-23.65 <sub>7</sub>	-42.64 <sub>8</sub>	-63.7 <sub>4</sub>
	323.15	-22.38 <sub>6</sub>	-40.22 <sub>14</sub>	-55.2 <sub>6</sub>
	343.15	-20.98 <sub>4</sub>	-38.3 <sub>13</sub>	-50.5 <sub>6</sub>
	van't Hoff eq		-41.7 <sub>6</sub>	

standard errors of the mean were estimated from these independent simulations.

Using GEMC, the Gibbs free energy for the transfer of a solute from the gas to liquid phase can be calculated directly from the number density ratio.<sup>9,10</sup>

$$\Delta G_{\text{trans}} = -RT \ln K_{\text{trans}} = -RT \ln \left( \frac{\langle \rho_{\text{liquid}} \rangle}{\langle \rho_{\text{gas}} \rangle} \right)_{\text{eq}} \quad (1)$$

where  $\langle \rho_{\text{liquid}} \rangle$  and  $\langle \rho_{\text{gas}} \rangle$  are the ensemble-averaged solute number densities (which are mechanical properties given in units of molecules per unit volume, Å<sup>3</sup>, or moles per 10<sup>-3</sup> m<sup>3</sup>) for the liquid and gas phases, respectively, at equilibrium. The variables  $R$  and  $T$  are the molar gas constant and absolute temperature.

The calculation of the enthalpy of transfer is more difficult because it requires the separate determination of the internal energies for the addition of a “single” solute to a large solvent bath for both phases. For each individual phase, the internal energy of solvation of a solute is equal to the difference between the total internal energy when the solute is in the phase (denoted as A) and the total energy when it is not (denoted as B)

$$U_{\text{solute}} = U_{\text{total}}^A - U_{\text{total}}^B \quad (2)$$

Since the internal energy is an extensive property, the solvent–solvent interactions dominate the total energy and a small difference between two large numbers needs to be determined. An often used approximation for pairwise-additive potentials is to assume  $U_{\text{solute-solvent}}^A = U_{\text{solute-solvent}}^B$  and to determine the internal energy of solvation using only the direct solute–solvent interactions,  $U_{\text{solute-solvent}}^A$ .<sup>11</sup> However, this approximation neglects the internal energy cost of the solvent reorganization caused by the presence of the solute. In the cases studied here, where the interest is on self-solvation (i.e., where the solute and solvent are identical species) and where helium, the majority component of the gas phase, does not partition strongly into any of the liquid solvents, the liquid phase is often pure solvent and the internal energy of (self-)solvation can be calculated from

$$U_{\text{solute}} = U_{\text{total}}/N \quad (3)$$

where  $N$  represents the total number of molecules in the liquid phase. The internal energy of solvation in the gas phase (being always a mixture consisting of solute and helium) needs to be calculated using eq 2. Although this causes a large relative uncertainty, the internal energy of solvation in the gas phase is small enough that it contributes very little to the internal energy

**TABLE 2: Heat Capacities of Transfer Calculated from Temperature Dependence of Enthalpies and Entropies**

solute	method	
	$(\partial H/\partial T)$ [J/mol·K]	$(\partial S/\partial \ln T)$ [J/mol·K]
<i>n</i> -octane	59 <sub>2</sub>	58 <sub>3</sub>
1-butanol	79 <sub>2</sub>	85 <sub>8</sub>
water	102 <sub>2</sub>	104 <sub>2</sub>

of transfer, which is calculated by taking the difference between the liquid and gas phases’ internal energies of solvation.

$$\Delta U_{\text{trans}} = U_{\text{solute}}^{\text{liquid}} - U_{\text{solute}}^{\text{gas}} \quad (4)$$

For the calculation of the enthalpy of transfer, the volumes of solvation (or partial molar volumes of the solute) have to be determined for each phase. These are calculated in a similar way as the solute’s internal energies.

$$V_{\text{solute}} = V_{\text{total}}^A - V_{\text{total}}^B \quad (5)$$

Again, the average volume can be used for configurations where the liquid phase is pure (as in eq 3). However, the volume of transfer is dominated by the gas-phase solvation volume. Fortunately, none of the solute molecules are found to aggregate appreciably in the helium gas phase under the conditions studied here. Therefore, the gas phase behaves nearly ideal, allowing us to use the overall molar volume of the gas phase to approximate the gas-phase solvation volume.

After obtaining the internal energies and volumes of solvation and using the Gibbs free energy of transfer, the enthalpy and entropy of transfer can be calculated from standard thermodynamic formulas.

$$\Delta H_{\text{trans}} = \Delta U_{\text{trans}} + p\Delta V_{\text{trans}} = (U_{\text{solute}}^{\text{liquid}} - U_{\text{solute}}^{\text{gas}}) + p(V_{\text{solute}}^{\text{liquid}} - V_{\text{solute}}^{\text{gas}}) \quad (6)$$

$$T\Delta S_{\text{trans}} = \Delta H_{\text{trans}} - \Delta G_{\text{trans}} \quad (7)$$

## Results and Discussions

The numerical values of the Gibbs free energies, enthalpies, and entropies of transfer for all three systems are summarized in Table 1. It is evident that  $\Delta G_{\text{trans}}$ ,  $\Delta H_{\text{trans}}$ , and  $\Delta S_{\text{trans}}$  decrease in magnitude over the temperature range of 75 K studied here, although the magnitudes of the decreases are small: about 5 kJ/mol for both  $\Delta G_{\text{trans}}$  and  $\Delta H_{\text{trans}}$  and about 20 J/mol·K for  $\Delta S_{\text{trans}}$ . However, it should be noted that the statistical errors for the individual values are substantially smaller than the differences between neighboring (in temperature) values of the transfer properties.

Under the assumption that the constant-pressure heat capacity of transfer,  $\Delta C_{p,\text{trans}}$ , remains constant over the temperature range studied here,  $\Delta C_{p,\text{trans}}$  can be estimated directly from either the temperature dependence of the enthalpy or the entropy.

$$\Delta H_{\text{trans}}(T_f) = \Delta H_{\text{trans}}(T_0) + \Delta C_{p,\text{trans}}(T_f - T_0) \quad (8)$$

$$\Delta S_{\text{trans}}(T_f) = \Delta S_{\text{trans}}(T_0) + \Delta C_{p,\text{trans}} \ln \left[ \frac{T_f}{T_0} \right] \quad (9)$$

A check on the reliability of the methods used to calculate enthalpies and entropies of transfer is the good agreement for the heat capacities of transfer calculated from eqs 8 and 9 (see Table 2). Immediately one should note that the heat capacities of transfer for *n*-octane and 1-butanol are about equal to their entropies of transfer, while  $\Delta C_{p,\text{trans}}$  exceeds  $\Delta S_{\text{trans}}$  for water.

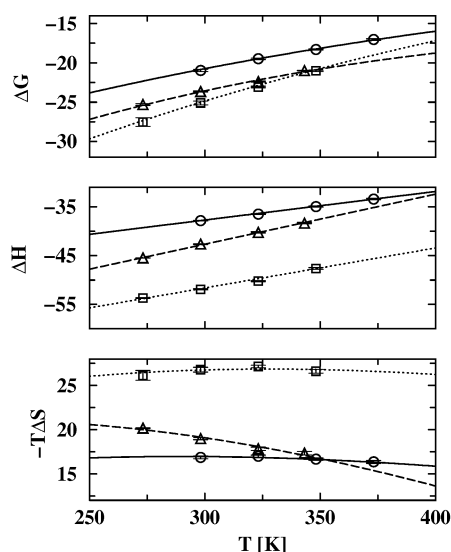


**Figure 1.** Gibbs free energies, enthalpies, and temperature–entropy values (all given in units of kJ/mol) as functions of temperature. The symbols depict the directly calculated values (eqs 1, 6, and 7), and the lines show fits using the averages of the constant-pressure heat capacities of transfer determined from the enthalpy or entropy derivatives (eqs 8 and 9) for *n*-octane (circles and solid lines), 1-butanol (squares and dotted lines), and water (triangles and dashed lines).

In Figure 1, the Gibbs free energies, enthalpies, and temperature–entropy values of transfer are plotted versus temperature together with their constant-pressure heat capacity fits to give a clearer picture of the temperature dependence of these values. The most important conclusion emerging from this figure is that the temperature dependence of the Gibbs free energy of transfer is dominated by the variation in the enthalpy of transfer with temperature for all systems and not by the temperature–entropy term, as one might assume from eq 7. For *n*-octane and 1-butanol, the product of temperature and entropy appears to be relatively constant over the temperature range studied; that is, the linear increase in temperature is offset by the decrease in the magnitude of the entropy of transfer. In contrast, the magnitude of the temperature–entropy term for solvation in water decreases with increasing temperature, thereby reducing the importance of this term for the Gibbs free energy of transfer.

Two points concerning the calculated values of the transfer properties require further discussion. First, it might appear somewhat unexpected that the values calculated for 1-butanol are lower (more negative) than those for the other two solvents. For the force fields used here, 1-butanol has the highest normal boiling point and the lowest vapor pressure. A lower vapor pressure results in a more negative value for  $\Delta G$ . The unusually large magnitude of 1-butanol's entropy of transfer may be explained by the fact that its solvation process requires the formation of a large cavity and a very specific local environment for the hydroxyl headgroup (see discussion of liquid structure). Furthermore, it should be noted that the calculated transfer properties for 1-butanol are in good agreement with experimental data at 298K:  $\Delta G = -25.8$  kJ/mol,  $\Delta H = -52.8$  kJ/mol, and  $\Delta S = -90.6$  J/mol·K.<sup>12</sup> Second, for water an unexpectedly large value is calculated for  $\Delta C_{p,trans}$  and the magnitude of the temperature–entropy term is found to decrease with increasing temperature. Experimental measurements<sup>3,12</sup> yield a much smaller value of  $\Delta C_{p,trans}$  of about 40 J/mol·K and a nearly constant value for  $T\Delta S$  of about  $-15$  kJ/mol. Clearly, the TIP5P water model, which yields excellent results for the specific density close to the temperature of the density maximum and for the liquid structure at ambient conditions,<sup>8</sup> is less suitable for simulations of phase equilibria and transfer properties. In particular, the temperature dependence of the transfer properties for the TIP5P model appears to be exaggerated and the normal boiling point and the critical temperature are substantially underestimated.

The observed temperature dependencies are caused by changes that occur in the liquid phases of the solvents. An increase of the temperature at constant pressure leads to a reduction in the solvent density and the cohesive energy density (Hildebrand solubility parameter),<sup>13</sup> which in turn lowers the internal energy of solvation in the liquid solvent. In addition, an increase in the temperature results in an increase of the compressibility factor of the solvent and a decrease of orientational order for polar fluids. The former reduces the entropic penalty associated with the creation of a cavity for the solute, while the latter reduces the entropic cost for solvent reorganization.

Figure 2 depicts pairwise radial-angular distribution functions that were calculated for the liquid phases of water and 1-butanol to investigate the temperature-induced changes in the structures

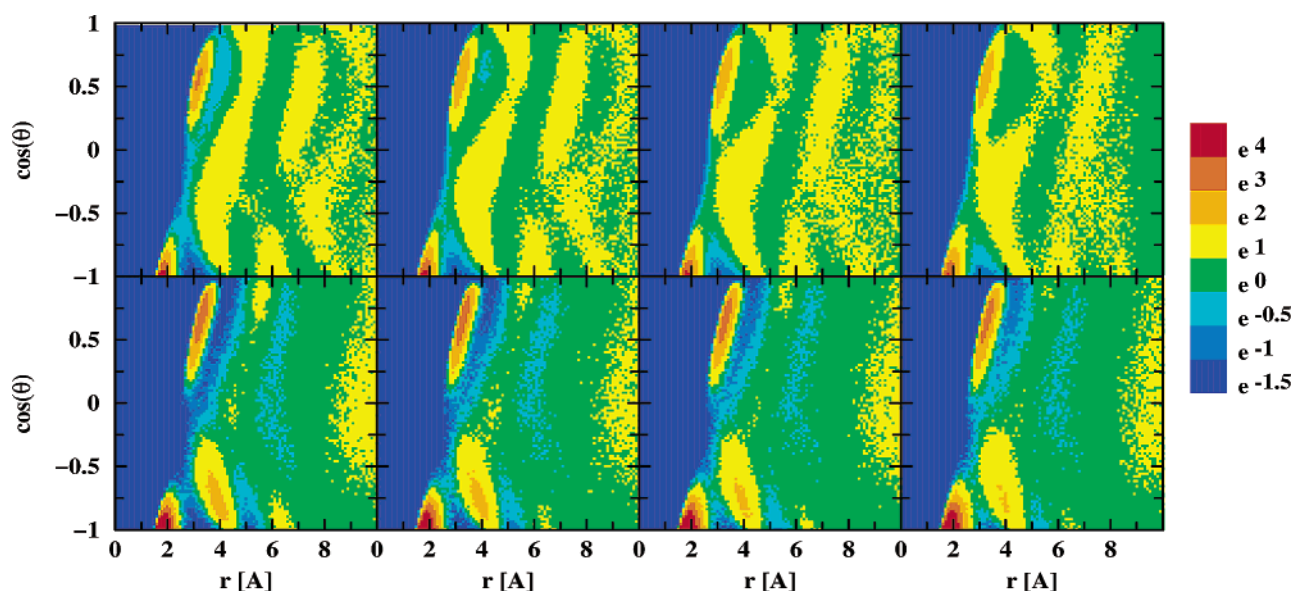


**Figure 2.** Two-dimensional radial-angular distribution surfaces normalized by the average density for water (top) and 1-butanol (bottom) shown for increasing temperature (from left to right).

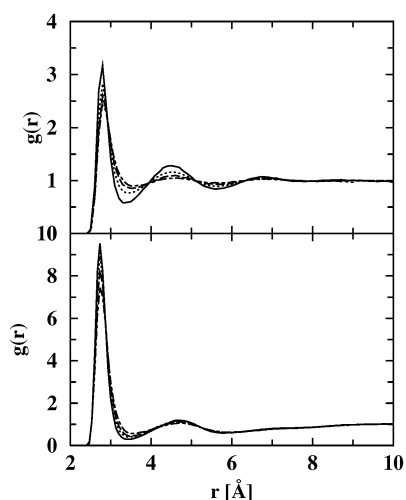


**Figure 3.** Temperature dependence of the oxygen–oxygen radial distribution functions for water (top) and 1-butanol (bottom). The solid and dashed–dotted lines depict the lowest and highest temperatures, respectively.

**TABLE 3: Normalized Differences in Radial Distribution Functions**

solvent	first peak	first valley	second peak	second valley
1-butanol	0.27	0.49	0.12	0.07
water	0.30	0.35	0.22	0.12

of these solvents. The radial part represents the distance (magnitude) of the “hydrogen-bond” vector from a polar hydrogen of molecule A to the oxygen of another molecule B. The angular part represents the angle between the “hydrogen-bond” vector and the hydrogen–oxygen bond vector of molecule A. Only the first peak ( $r_{\text{OH}} \approx 2 \text{ \AA}$  and  $\cos \theta < -0.7$ ) corresponds to a hydrogen bond. The second peak ( $r_{\text{OH}} \approx 3 \text{ \AA}$  and  $\cos \theta \approx 0.6$ ) originates from the other hydrogens of a hydrogen-bonded pair of molecules that are not involved in the original hydrogen bond. The other peaks and bands are associated with the second and higher solvation shells. The intensity of the first peak is much larger for 1-butanol than for water; that is, the formation of hydrogen-bonded clusters found in 1-butanol requires substantial reorganization and leads to a microheterogeneous structure. The loss of features (reduction in peak heights and valley depths) observed in the radial-angular distribution functions for water and 1-butanol demonstrates that both solvents disorder with increasing temperature. Oxygen–oxygen radial distribution functions for water and 1-butanol are shown in Figure 3. In agreement with the radial-angular distribution functions, it is evident for 1-butanol that hydrogen-bonded clusters persist at the higher temperature and that most of the decrease in order appears to be short-ranged, i.e., limited to the first peak and first valley, whereas this is not the case for water, for which the structures of the second and third solvation shells are almost completely lost at the highest temperature. To quantify the changes in the RDFs, the percentage change in peak/valley heights/depths ( $|\mathcal{G}_{\text{high}T}(r) - \mathcal{G}_{\text{low}T}(r)|/\mathcal{G}_{\text{low}T}(r)$ ) is given in Table 3. The large change in the long-range ordering that is only observed for liquid water is likely the basis for the stronger temperature dependence of the entropy of transfer found for water; that is, the temperature dependence of the entropy of transfer is stronger than linear for water and  $T\Delta S$  decreases in magnitude with increasing temperature. It should be emphasized that this finding might be strongly coupled to the deficiencies of the TIP5P water discussed above.

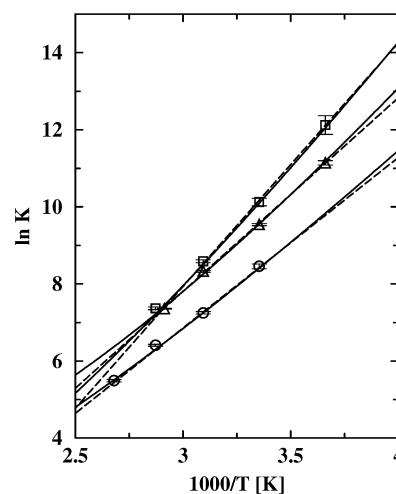


**Figure 4.** Van’t Hoff plots showing linear fits (dashed lines) and constant-pressure heat capacity fits (solid lines) for *n*-octane (circles), 1-butanol (squares), and water (triangles).

By combining eqs 1 and 7, the van’t Hoff equation can be derived.

$$\ln K_{\text{trans}}(T) = -\frac{\Delta H_{\text{trans}}(T)}{RT} + \frac{\Delta S_{\text{trans}}(T)}{R}$$

$$\frac{d \ln K_{\text{trans}}(T)}{d(1/T)} = -\frac{\Delta H_{\text{trans}}(T)}{R} \quad (10)$$

If enthalpy and entropy are assumed to be constant over the temperature range of interest, then a plot of  $\ln K_{\text{trans}}$  versus  $T^{-1}$  should result in a straight line, the slope of which is the enthalpy of transfer. In Figure 4, linear fits (eq 10) and fits using the constant-pressure heat capacities of transfer (eqs 8 and 9) for the calculated partition constants are compared. Clearly, the differences between the linear and curved fits are very small, and the precision of the simulation data is not sufficient to argue that the fits using the heat capacities are better. The curvature induced by the heat capacity of transfer is too small to cause significant departures from linear behavior over the temperature range investigated here, a result that is also reflected in the quality of Clausius–Clapeyron fits to saturated vapor pressure data. The enthalpies of transfer approximated from the van’t Hoff equation for *n*-octane, 1-butanol, and water are  $-36.8 \pm 1.1$ ,  $-49.0 \pm 2.2$ , and  $-41.7 \pm 0.6 \text{ kJ/mol}$ , respectively, as given in Table 1. Thus, the van’t Hoff equation predicts enthalpies of transfer in the range of the directly calculated  $\Delta H_{\text{trans}}$  (eq 6), but the uncertainties in the van’t Hoff enthalpies are about an order of magnitude larger than those from eq 6. Of course, the van’t Hoff equation will in principle yield the correct answer for an infinitesimal change in temperature, but the uncertainties inherent in both the experimental determination and the calculation (via eq 1) of the partition constants necessitate finite temperature changes. The problem that even small uncertainties in the partition constants preclude the observation of curvature in van’t Hoff plots has been recently discussed by Chaires using simulated equilibrium constants with prescribed amounts of statistical noise.<sup>14</sup>

## Conclusions

Simulations in the Gibbs ensemble were used to investigate the temperature dependence of the thermodynamic transfer properties for self-solvation of *n*-octane, 1-butanol, and water.



The simulations demonstrate that the temperature dependence of the Gibbs free energies of transfer is mainly driven by the changes in the enthalpies of transfer, that is, the heat capacities of transfer. In contrast, the changes in the temperature–entropy terms are small because the increase in the temperature is compensated by a decrease in the entropies of transfer. The decrease in the magnitudes of the enthalpies and entropies of transfer with increasing temperature can be explained by the decrease in cohesive energy densities of the liquid phases and a reduction in the entropic penalties for cavity formation and solvent reorganization.

Despite the large temperature dependence of the enthalpy of transfer, van't Hoff fits describe the calculated partition constants remarkably well and the van't Hoff enthalpies of transfer are in good agreement with the directly calculated values near the average temperature. Gibbs free energies of transfer or partition constants with extremely small uncertainties (less than 0.01 kJ/mol or 0.5%) would be required to unambiguously observe heat capacity effects in van't Hoff plots over the range of temperatures studied here.

Finally, the fact that the heat capacities and entropies for vapor-to-liquid transfers are comparable in magnitude should serve as a warning for the use of linear extrapolations of free energies over a wide range of temperatures, as is often done when using the concept of entropy–enthalpy compensation.<sup>15</sup> However, it can be expected that heat capacities for liquid-to-liquid transfers will be significantly smaller than those observed here for the vapor-to-liquid transfers because in the former case the changes in cohesive densities and compressibility factors with temperature for the two liquid phases will at least partially compensate each other.

**Acknowledgment.** We thank Peter Carr for many stimulating discussions. Financial support from the National Science Foundation (CHE-0213387 and CTS-0138393) and a Depart-

ment of Energy Computational Science Graduate Fellowship (C.D.W.) is gratefully acknowledged. Part of the computer resources were provided by the Minnesota Supercomputing Institute.

## References and Notes

- (1) Baldwin, R. L. *Proc. Natl. Acad. Sci. U.S.A.* **1986**, *83*, 8069.
- (2) Naghibi, H.; Tamura, A.; Sturtevant, J. M. *Proc. Natl. Acad. Sci. U.S.A.* **1995**, *92*, 5597. Holtzer, A. *Biopolymers* **1997**, *42*, 499.
- (3) Bloomfield, V. A.; Rouzian, I. *Biophys. J.* **1999**, *77*, 3242.
- (4) Ben-Naim, A. *Solvation Thermodynamics*; Plenum: New York, 1987.
- (5) Giddings, J. C. *Dynamics of Chromatography*; Marcel Dekker: New York, 1965.
- (6) (a) Panagiotopoulos, A. Z. *Mol. Phys.* **1987**, *61*, 813. (b) Panagiotopoulos, A. Z.; Quirke, N.; Stapleton, M.; Tildesley, D. J. *Mol. Phys.* **1988**, *63*, 527.
- (7) (a) Siepmann, J. I.; Frenkel, D. *Mol. Phys.* **1992**, *75*, 59–70. (b) Frenkel, D.; Mooij, G. C. A. M.; Smit, B. *J. Phys.: Condens. Matter* **1992**, *4*, 3053–3076. (c) Martin, M. G.; Siepmann, J. I. *J. Phys. Chem. B* **1999**, *103*, 4508–4517.
- (8) (a) Martin, M. G.; Siepmann, J. I. *J. Phys. Chem. B* **1998**, *102*, 2569. (b) Chen, B.; Potoff, J. J.; Siepmann, J. I. *J. Phys. Chem. B* **2001**, *105*, 3093.
- (9) Mahoney, M. W.; Jorgensen, W. L. *J. Chem. Phys.* **2000**, *112*, 8910.
- (10) Ben-Naim, A. *J. Phys. Chem.* **1978**, *82*, 792.
- (11) (a) Martin, M. G.; Siepmann, J. I. *Theor. Chem. Acc.* **1998**, *99*, 347. (b) Martin, M. G.; Zhuravlev, N. D.; Chen, B.; Carr, P. W.; Siepmann, J. I. *J. Phys. Chem. B* **1999**, *103*, 2977. (c) Chen, B.; Siepmann, J. I. *J. Am. Chem. Soc.* **2000**, *122*, 6464.
- (12) Wick, C. D.; Siepmann, J. I.; Klotz, W. L.; Schure, M. R. *J. Chromatogr. A* **2002**, *954*, 181.
- (13) (a) Smith, B. D.; Srivastava, R. *Thermodynamic Data for Pure Compounds: Part A Hydrocarbons and Ketones; Thermodynamic Data for Pure Compounds: Part B Halogenated Hydrocarbons and Alcohols*; Elsevier: Amsterdam, 1986. (b) NIST Chemistry WebBook available at <http://webbook.nist.gov/chemistry/>.
- (14) Rowlinson, J. S.; Swinton, F. L. *Liquids and Liquid Mixtures*; Butterworth: London, 1982.
- (15) Chaires, J. B. *Biophys. Chem.* **1997**, *64*, 15.
- (16) (a) Boots, H. M. J.; de Bokx, P. K. *J. Phys. Chem.* **1989**, *93*, 8240. (b) Li, J.; Carr, P. W. *J. Chromatogr. A* **1994**, *670*, 105. (c) Vailaya, A.; Horváth, C. *J. Phys. Chem. B* **1998**, *102*, 701.